Bioconjugate Chemistry

Article

pubs.acs.org/bc

Controlled Assembly of Artificial Protein–Protein Complexes via DNA Duplex Formation

Eliza Płoskoń,*[,†] Sara C. Wagner,[†] Andrew D. Ellington,[‡] Michael C. Jewett,[§] Rachel O'Reilly,[∥] and Paula J. Booth*[,†,⊥]

[†]School of Biochemistry, University of Bristol, University Walk, Bristol BS8 1TD, United Kingdom

[‡]Institute for Cellular and Molecular Biology, Center for Systems and Synthetic Biology, Department of Chemistry and Biochemistry, University of Texas at Austin, Austin, Texas 78712, United States

[§]Chemical and Biological Engineering, Chemistry of Life Processes Institute, Northwestern University Evanston, Illinois 60208, United States

[∥]Department of Chemistry, University of Warwick, Coventry, West Midlands CV4 7AL, United Kingdom

[⊥]Department of Chemistry, King's College London, 7 Trinity Street, London SE1 1DB, United Kingdom

Supporting Information

ABSTRACT: DNA–protein conjugates have found a wide range of applications. This study demonstrates the formation of defined, non-native protein–protein complexes via the site specific labeling of two proteins of interest with complementary strands of single-stranded DNA in vitro. This study demonstrates that the affinity of two DNA–protein conjugates for one another may be tuned by the use of variable lengths of DNA allowing reversible control of complex formation.

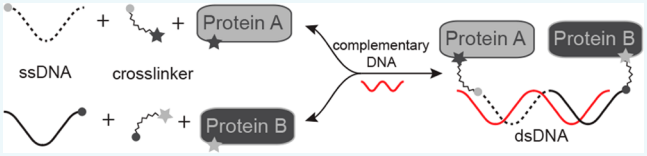

INTRODUCTION

The design and construction of novel biologically based materials and processes is motivated in large part by the diverse range of applications and the real-world impact they can have on the fields of metabolic engineering, chemical biology, synthetic biology, and biocatalysis.[1] In these fields, there is an appreciation that it must be possible to direct and generate artificial multiprotein complexes.[2] Natural proteins work in concert with one another in multiprotein complexes to enable their intricate functions. The ability to mimic such multiprotein organization by forming tailored, artificial protein–protein complexes is therefore an important challenge. As an example, the potential for such complexes in biocatalysis has been proposed previously.[3]

The synergistic abilities of DNA and proteins have been exploited for the generation of biomacromolecular hybrids with a range of applications ranging from the fabrication of nanostructured materials,[4] synthetic energy transfer devices, to tools for imaging and diagnostics.[5] Each of these approaches are based upon the remarkable ability of short ssDNA to recognize and bind to their complementary strand and, thus, to direct the assembly of the proteins.

Motivated by a variety of ongoing research projects within our group, including the study of membrane and membrane associated proteins and the generation of novel self-assembly materials, we sought a convenient way of generating specific, yet noncovalent, complexes between proteins. There are some notable previous successes in this area. DNA-mediated assembly has been used by a number of groups to bring proteins together at both the surface of solid supports and in solution. Examples include DNA immobilization at the surface of a gold electrode to drive the formation of a complex between DNA-conjugated MP11[6] and DNA-conjugated GOX, the use of a DNA hairpin to bring two isolated subdomains of Cytochrome P450 BM3 together, thus reconstituting the active enzyme,[7] as well as the use of hinged DNA to allow the assembly of enzyme cascades in a topologically controlled manner.[8] Although powerful, these methods, however, hinder certain applications. Our design aims for the complexes were as follows (Figure 1a): (1) They should allow two proteins to be brought together. (2) These complexes should be extensible—with the potential that more proteins (or other cargoes—such as polymers) may be added to the system. (3) The complexes should be reversible, offering bidirectional control of complex formation. (4) Our design should not involve physical absorption or chemical coupling to a solid support (to minimize the loss of native conformation).

Three designs were pursued in this work. For two of our designs it was proposed that two, normally noninteracting proteins could be forced to form a complex with one another by conjugating each to strands of ssDNA and then using a complementary strand of ssDNA to bring the proteins together (as illustrated schematically in Figure 1b and c). It is envisioned in Design A that extra components may be added to the system by inclusion at the ends of the complementary linker strand with a length of about 7 nm. In this design the distance

Received: October 15, 2014
Revised: January 15, 2015
Published: January 20, 2015

DOI: 10.1021/bc500473s
Bioconjugate Chem. 2015, 26, 427–434

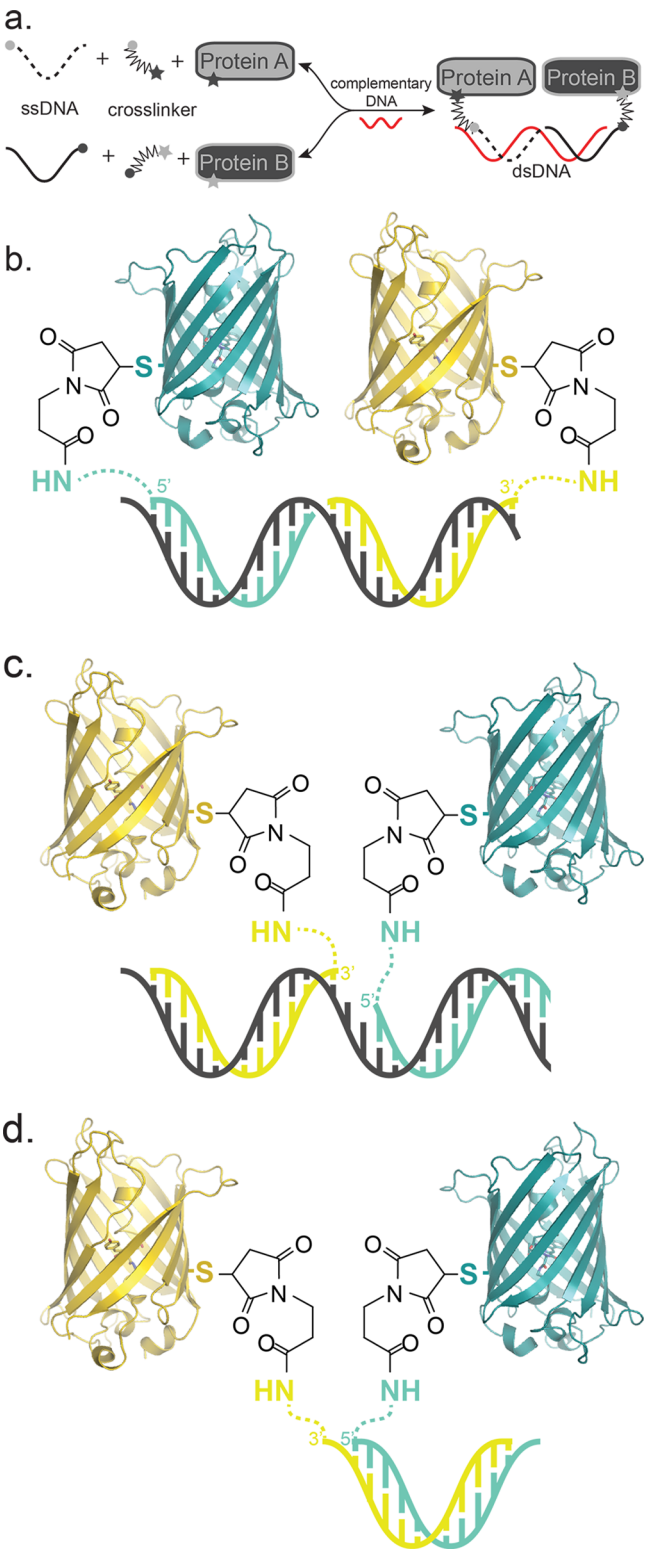

Figure 1. a. General scheme for designed method. Schematic of the proposed designs. In designs A and B, ssDNA-ECFP and ssDNA-EYFP are brought together by a complementary ssDNA linker. b. Design A is orientated so that the proteins are at the ends of the complex. c. Configuration where ECFP and EYFP are brought together in the center of the DNA complex. d. In Design C the proteins are brought together by complementary ssDNA strands of DNA.

between the proteins could reach 9 to 10 nm when the DNA modifiers and cross-linkers are taken into account. In Design B, extra components may conceivably be included at both the free terminal of the ssDNA conjugated to the target protein and each end of the complementary linker ssDNA, with the proteins approximately 4 to 6 nm apart. These designs have precedence in the work of Erkelenz et al., who used looped DNA to bring together and control enzyme complex formation,[7] and to the work of Gholami et al., who used peptide nucleic acid protein conjugates to dimerize fluorescent proteins.[9] Finally, a more direct approach is proposed in our third Design C (Figure 1d), with both proteins being labeled directly with complementary strands of ssDNA so that the two proteins are brought adjacent to one another to the distance of no greater than 4 nm. In such an arrangement extra components may be considered at the free terminal of the ssDNA conjugated to the target protein.

In pursuit of our reversibility criterion, we sought to take advantage of the thermal melting of DNA complexes. Hybridization of ssDNA to form dsDNA duplexes shows high thermodynamic stability. Consequently, the lengths of oligonucleotide DNAs that may be used are limited to those with melting temperatures (T_m, defined as the temperature at which 50% of the dsDNA is denatured) low enough that the protein cargo is not denatured during DNA melting. Most work to date (such as the work of Erkelenz or Gholami) uses oligonucleotides of approximately 20 bp or higher to ensure complex formation. Such lengths stabilize duplex formation greatly and thus result in melting temperatures typically on the order of 50−60 °C, making such oligonucleotides unsuitable in this work. We thus targeted complex formation using short oligonucleotides with a maximum T_m of approximately 30 °C.

In order to bring the proteins in close proximity, a number of DNA architectures have been explored in this work. These have been designed based on two DNA architectures that are commonly employed in DNA templated synthesis to enable multistep oligomer formation, the omega (Designs A and B) and end-of-helix architectures (Design C).[10] The omega architecture utilizes short DNA sequences which are attached to the protein, and these bind to different portions of a linear template, either at opposite ends of the template (Design A) or across a nick (Design B). It has been demonstrated that the number of base pairs across the nick has an effect on the efficiency of transfer between the strands,[11] and indeed the end of helix architecture has been proposed to be the most efficient in DNA template chemistries.[12,13]

Our model proteins of choice were the fluorescent proteins ECFP and EYFP. These enable the facile detection of complex formation using Forster resonance energy transfer (FRET) at low concentrations with high sensitivity. Moreover, FRET permits the complex state to be monitored at a range of temperatures not easily studied by traditional techniques in the field such as gel-shift assays and size exclusion chromatography. In one recent example, Gholami et al. used FRET to verify heterodimer assembly induced using a DNA template.[14] Green fluorescent protein (GFP) and its derivatives such as ECFP and EYFP can form homodimers both in solution and in crystals with a dissociation constant of approximately 100 μM.[15] This tendency of GFP to weakly interact with itself is attributed to a conserved hydrophobic patch on the protein surface. Therefore, to eliminate spurious FRET signaling of the DNA−protein complexes via ECFP-EYFP aggregation, the point mutation

DOI: 10.1021/bc500473s
Bioconjugate Chem. 2015, 26, 427−434

A206 K which abrogates formation of the weak dimer via charge repulsion was introduced into both proteins.[16]

In this short report we describe the construction of a thermally controlled protein complex using covalent single-stranded DNA (ssDNA) conjugates of the fluorescent proteins ECFP and EYFP.

RESULTS

Design. The successful formation of the desired complex depends on positioning the linker on the surface of protein and selection of an appropriate functional group for conjugation. Previously, Niemeyer attempted to cross-link EYFP to ssDNA while first protecting the thiol groups of the protein.[17] This was found to lead to a complex mixture of products with different stoichiometries of DNA−protein and uncleaved protecting groups. In light of this, Niemeyer et al. changed their approach and created a monocysteine containing mutant of GFP, which they could label in a stoichiometric fashion.[17] We also used maleimide conjugation to Cys and first investigated the reactivity of the native Cys residues 48 and 70. We found that Cys70 (buried) of EYFP and ECFP did not to react under our experimental conditions, while the partially surface exposed Cys48 had low reactivity (data not shown); these observations are consistent with the findings of Inouye and Tsuji.[18] Consequently, the surface exposed Cys48 was mutated to alanine and an alternative cysteine (residue 34 in both ECFP and EYFP) in a more exposed position was introduced. This approach enables specific covalent-linking in close proximity to the fluorophore, and prevents or limits the formation of undesired byproducts.[19]

ssDNA Protein Conjugation. ssDNA was conjugated to the proteins involved, using the heterobifunctional linker BMPS. Specifically, amino modified ssDNA oligonucleotides were first reacted with *N*-β-Maleimidopropyl-oxysuccinimide ester (BMPS) to generate thiol-reactive maleimide-ssDNA which was in turn used to conjugate to the mutants of ECFP and EYFP bearing Cys34. SDS PAGE and MALDI mass spectrometry was used to confirm the monofunctionalization of the protein (Supporting Information Figures S1 and S2, respectively). No evidence for multiple additions was observed. Attachment of the ssDNA did not alter the fluorescent properties of the proteins. UV spectroscopy of the samples is consistent with the length of the DNA fragment attached, as the shorter the DNA attached, the higher the Abs (430 or 510)/Abs 254 ratio (Supporting Information Table S3).

Monitoring Complex Formation. Once prepared, the ability of the ssDNA−protein conjugates to form the desired hybrids via complementary base pairing was tested. Consistent with previous published work in the field, we used a combination of size exclusion chromatography, dynamic light scattering (DLS), gel shift assays, and fluorescence methods to observe complex formation. In each case, the complexes were hybridized together in PBS buffer (pH 7.4).

To increase the probability of the proteins being placed on the same side of the dsDNA, while minimizing the length of the DNA fragments used (to minimize the melting temperature), in designs A and B we designed the linker to reach two full turns of DNA helix. Thus, in our model system for design A, 10 base pair (bp) ssDNA-ECFP and 11 bp-ssDNA-EYFP were hybridized to a 21 bp complementary ssDNA strand.

In Design B, the donor and acceptor are expected to be placed closer to one another, potentially aiding the observation of FRET between the two fluorophores. Cognizant of the risk of steric clashes between the two proteins interfering with complex formation, we introduced two additional base pairs between the protein linked DNA fragments; lengthening the linking complementary ssDNA to 23 bp compared to the linker length used in Design A.

In Design C, an alternate approach is taken where the proteins are placed at the same end of a DNA double helix where one protein is attached to the 5′ end of one strand and the second protein is placed on the 3′ end of a complementary strand (as illustrated Figure 1d). In our initial experiments complex formation between complementary 10bp-ssDNA linked ECFP and EYFP proteins was assayed.

Fluorescence Studies. A FRET based assay was used as an initial screen of complex formation by each design. ECFP and EYFP are widely used as a FRET pair in both in vivo and in vitro studies due to the large overlap of the EYFP absorption and ECFP emission (see Supporting Information Table S2).[20] As can be seen from Supporting Information Figure S3, however, EYFP (the acceptor) fluoresces when excited at 433 nm, which is the maximum excitation wavelength for ECFP (the donor). This emission from EYFP when excited at 433 nm would obscure, or complicate, any emission arising from FRET between the two fluorophores. Thus, in the FRET experiments presented, the ECFP fluorescence was excited at 400 nm wavelengths to prevent this crosstalk-excitation of the EYFP, ensuring that any observed emission at the λ_{max} of EYFP (527 nm) arises through FRET between ECFP and EYFP and not through direct excitation of the EYFP.

FRET experiments were further complicated in this study by the temperature dependence of both ECFP and EYFP fluorescence. This is important, as key experiments in this work involve the thermal melting of the hybridized dsDNA to disassemble the complex selectively. ECFP and EYFP show temperature-dependent fluorescence changes (Supporting Information Figure S4). With ECFP, the lower the temperature, the greater the fluorescence emission with its intensity inversely proportional to temperature and with about 40% of its fluorescence emission intensity being lost between 2 and 52 °C. In contrast, EYFP's fluorescence intensity increases with temperature, peaking at between 25 and 30 °C, and then drops as the temperature is raised further.

Design A: ECFP and EYFP Placed at the Ends of Linking DNA. Pursuing Design A (outlined in Figure 1b), we attempted to observe the formation of the target complex between the 10bp-ssDNA-ECFP and 11bp-ssDNA-EYFP hybridized to a 21 bp complementary ssDNA strand. Equimolar (0.5 μM) amounts of 10bp-ssDNA-ECFP and 11bp-ssDNA-EYFP conjugates were mixed and incubated along with an equimolar amount of the complementary linker DNA. As a control experiment, noncomplementary ssDNA was used of the same length (21 bp) as the joining linker. To minimize concentration effects, the mixture of the ssDNA−protein conjugates was divided between the actual experiment and the control sample prior to the addition of the appropriate specific or unspecific DNA. Prepared samples were incubated at 50 °C for 2 min and then equilibrated to room temperature to allow the DNA strands to complement one another. Fluorescence excitation was recorded at 20 °C at 400 nm (Figure 2a). No increase in emission at 527 nm from the ECFP is observed, however, which would correspond to FRET between the two protein fluorophores.

Design B: ECFP and EYFP Placed in the Middle of Linking DNA. Having failed to observe FRET between the two proteins

DOI: 10.1021/bc500473s
Bioconjugate Chem. 2015, 26, 427−434

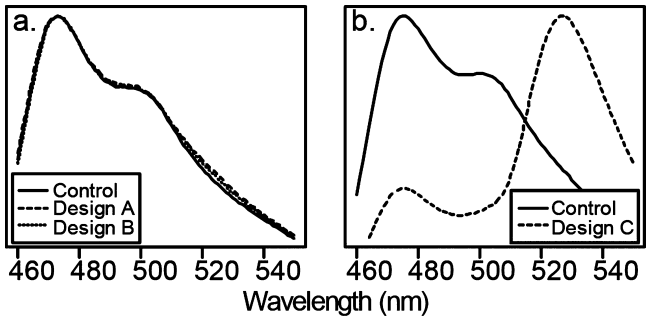

Figure 2. Fluorescent emission spectra (excitation 400 nm, normalized to maximium intensity) recorded at 20 °C on an equimolar (0.5 μM) mixtures of a. Design A: ECFP and EYFP attached to 10 bp and 11 bp ssDNA, respectively, in the presence of 21 bp complementary linker (from Design A). Design B: ECFP and EYFP attached to 10 bp and 11 bp ssDNA, respectively, in the presence of 23 bp complementary linker (from Design A). Control with noncomplementary DNA fragment (21 bp). b. ECFP and EYFP attached to 10 bp complementary (Design C) and noncomplementary ssDNA fragments. In the control, the proteins are conjugated with noncomplementary DNA. A strong emission at 527 nm is observed arising from FRET between the EYFP and ECFP when proteins are joined by complementary DNA, but not when conjugated with the noncomplementary DNA strands.

by using Design A, we pursued our second design (Figure 1c) where we attempted to place both proteins together in the middle of the linking DNA. Emission spectra were recorded for this combination and a control in the presence of a noncomplementary strand of ssDNA of equal length as described previously. Figure 2a presents the intensity normalized spectra obtained for this configuration. As with Design A, the fluorescence emission (when excited at 400 nm) of EYFP is quenched in the presence of the complementary linker compared to the control with no linker DNA present and no FRET between the two protein fluorophores is observed.

Design C: Alternative Design Strategy. In Design C, the complex is designed such that the proteins are adjacent to one another at the same end of a DNA (as illustrated Figure 1d). Figure 2b shows the emission spectra recorded for equimolar ECFP and EYFP attached to complementary DNA fragments of 10 bp. When these two proteins are allowed to hybridize with one another a strong FRET is observed with an emission of the EYFP acceptor at 527 nm confirming the formation of a complex. Importantly, controls with proteins linked to noncomplementary ssDNA of the same lengths do not show FRET. Thus, the FRET relies upon the specific interaction of the complementary ssDNA strands bringing together the two fluorescent proteins.

DNA binding may be altered by the presence of metal ions. The addition of the divalent metal ions Mg^{2+} and Zn^{2+}, however, had no effect on the degree of FRET observed in Designs A, B, and C (Supporting Information Figure S6). Under these conditions, some quenching of the fluorophore is observed.

Effect of ssDNA Length on Design C Stability. With the success of Design C in forming the desired protein−protein complex and enabling strong FRET to be observed, we sought to test the effect of varying the length of DNA linkers to establish the minimum length of DNA that can be used to drive protein complex formation and the effect of DNA length on the thermal stability of the complex. Ten, seven, and five base-pair-long dsDNA strands with 24, 17, and 12 H-bonds, respectively, were tested. In these experiments, we took advantage of the concentration dependence of FRET—where the lower complex present results in less transfer and thus lower emission intensity.

Figure 3 shows the effect of different lengths of conjugated ssDNA on the stability of the complex. The significant emission

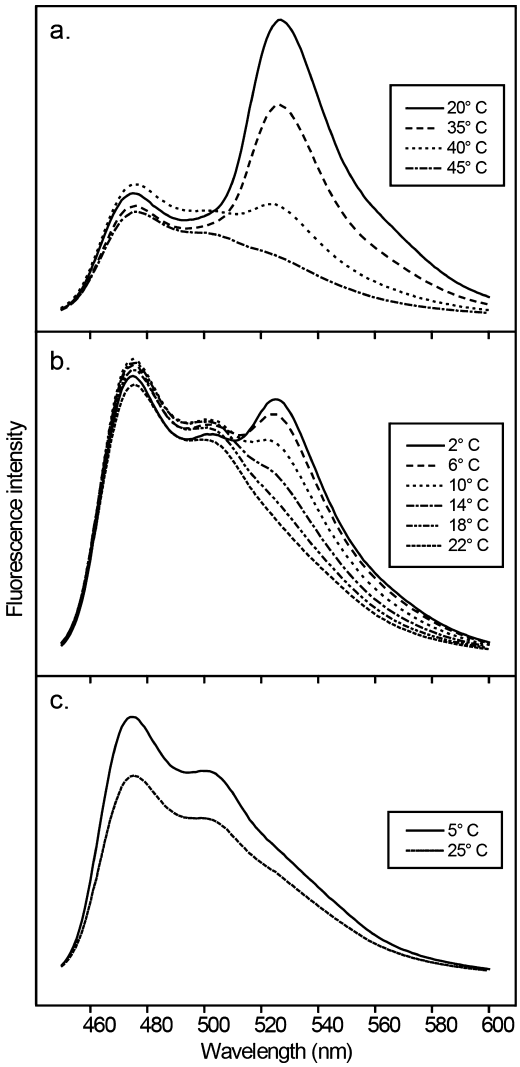

Figure 3. Emission spectra (excitation 400 nm) recorded on an equimolar mixture of ECFP and EYFP attached to complementary DNA fragments of different lengths in Design C. Overlaid spectra at different temperatures are shown. a. Proteins are linked with 10 bp complementary ssDNA strands which result in strong FRET signal observed at 527 nm at 20 °C, which decreases as the temperature is raised. b. Proteins are linked to 7 bp complementary ssDNA which results in a less prominent FRET signal at 527 nm, which also decreases with increasing temperature. c. Proteins are linked to 5 bp complementary ssDNA. No FRET emission is observed.

band at 527 nm in Figure 3a clearly indicates Förster resonance energy transfer between the ECFP and EYFP at temperatures of 20 and 35 °C with a 10 bp linker. Figure 3b also shows FRET with the 7 bp linker, but of lower intensity and at lower temperatures. Thus, there is a larger population of the associated complex formed with the 10 bp linker as observed by the higher FRET intensity. Energy transfer yield estimated from donor emission at 4 °C for 10 bp and 7 bp linkers was 0.6 and 0.4, respectively. No emission at 527 nm is observed in the

DOI: 10.1021/bc500473s
Bioconjugate Chem. 2015, 26, 427−434

case of the 5-bp-long ssDNA fragment even at 5 °C. Thus, the 12 H-bonds in the 5 bp dsDNA is insufficient to hold together the complex at any of the temperatures tested. A decrease in fluorescence is observed in Figure 3c as the temperature increases, in line with the temperature-sensitive fluorescence of the ECFP donor.

The populations of these complexes at low temperature are consistent with the decreasing stability of the complexes as the length of DNA is shortened, as indicated by predictions of their ΔG and T_m made using OligoCalc.[21] It is important to note that the calculation of thermodynamic parameters for short DNA fragments is difficult. The authors of OligoCalc note that the oligonucleotide sequence should be at least 8 bases long to allow an accurate T_m to be calculated.[21] This limitation arises, in part, from the lower propensity of shorter DNA fragments to form secondary structure, thus lowering their T_m further.

As the temperature increases, it is expected that the equilibrium shifts toward the dissociated monomers and the dsDNA melts, removing the spatial proximity of the proteins and consequently stopping the FRET. Figure 3a shows the melting profile of the 10 bp linked complex as monitored by FRET. The predicted T_m for this dsDNA is 30 °C. Consistent with this melting temperature, as the temperature is increased from 20 to 45 °C the FRET signal decreases. No FRET is observed at 45 °C, consistent with the complex being fully dissociated at this temperature. At the T_m, it is expected that half of the dsDNA present should be melted. We observe, however, slightly less than a 50% drop in FRET at this temperature compared to FRET at 20 °C. We believe this to be due either to a stabilizing effect brought on by the presence of the two proteins or possible inaccuracies in the oligonucleotide T_m predictions for short lengths of dsDNA. We note little change in the ECFP emission which is due to the previously noted temperature dependence on ECFP fluorescence. It was found that 17 H-bonds (7 bp DNA) were capable of sustaining hybridization only at low temperatures with the complex completely melted at room temperature (Figure 3b).

As only one of our designs showed the desired FRET behavior, we revisited them with other biophysical techniques to confirm or refute complex formation.

Fluoresence Titration. We began by monitoring the formation of the omega complexes, Designs A and B, which showed no-FRET using a fluorescence titration assay where we observed the quenching of the fluorophores upon titration with the complementary linker DNA. This revealed rapid quenching of the fluorophore in Design A as the amount of linker was increased; consistent with the formation of a complex. We found that in the design A the binding of DNA linker is saturated when the equimolar ratio of DNA liner in relation to ECFP and EYFP is reached (Supporting Information Figure S7). Although some quenching of the Design B fluorophores was observed upon titration with the linker DNA, this was considerably less than seen with Design A and is comparable to a water-only control.

Gel Shift Assay. Next, we analyzed each complex by native PAGE (4–20% gradient acrylamide) as shown in Figure 4. Conjugation of the protein with DNA increased the electrophoretic mobility of the species compared to the unmodified proteins (data not shown) due the significant increase in net negative charge afforded by the addition of the ssDNA to the proteins with only a marginal increase in size (Stokes radius). Designs A and C are both observed to display reduced electrophoretic mobility compared to a nonhybridized control,

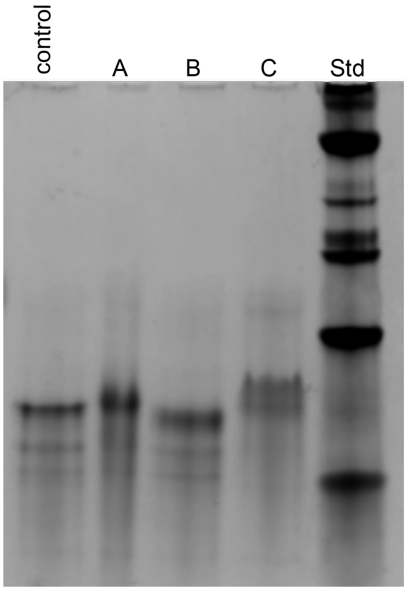

Figure 4. Gel shift assay. Control is a mixture of 10 bp ECFP and 11 bp EYFP with 21 bp noncomplementary linker. a. Design A shows reduced electrophoteric mobility compared to the control consistent with the presence of a larger species. b. Design B shows increased electrophoretic mobility consistent with an increase in charge but with little or no increase in size. c. Design C shows a number of bands, the lowest of which has a similar mobility to the presumed dimer in complex A. Standard is NativeMark Unstained Protein Standard - Life Technologies. Note: the standard is designed for the analysis of globular proteins and is not informative given the highly charged nature of the DNA–protein conjugates.

consistent with the formation of a complex of greater size. In this experiment, Design C appears as a notably broader band possibly suggesting a larger complex or mixture of states. The lowest band observed in Design C has a similar electrophoretic mobility as the presumed heterodimer-complex in Design A. Meanwhile, Design B shows increased electrophoretic mobility in line with a species of increased net negative charge.

Size Exclusion Chromatography. The size of the resulting complexes was assessed qualitatively by size exclusion chromatography (SEC, Supporting Information Figure S8). The unmodified EYFP and ECFP elute from a Superdex 200 (10/300) SEC column in 15.8 mL. Upon conjugation of these proteins with the 10 bp ssDNA, a decrease in retention time is observed (15.3 mL) consistent with an increase in Stokes radius due to the modification. In Design A, a new peak is observed at 12.3 mL upon hybridization of the complex. In Design B, a single peak is observed at 14 mL, and in Design A, a small peak of similar retention time is observed. The results however for Design C are ambiguous. In addition to the formation of a new peak which elutes after 13 mL, which we ascribe to the dimer of the two proteins, upon hybridization a broad peak is also observed; this begins to elute after 8.5 mL and stretches over the next 3 mL. This result fits with the larger species suggested by the gel-shift assay.

Dynamic Light Scattering. To clarify the nature of the complex formed by Design C, the size of the species present in each complex was determined by DLS on 10 μM samples in PBS buffer (Supporting Information Figure S9). DLS reveals that Design A forms a complex of approximately twice the size of the monomeric protein (118 ± 39 kDa and 41 ± 16 kDa, respectively) consistent with the formation of the hetero-

DOI: 10.1021/bc500473s
Bioconjugate Chem. 2015, 26, 427–434

dimeric complex. Design B, however, is increased in mass compared to the monomeric control, but is an intermediate value (67 ± 67 kDa) between the monomer and the presumed heterodimeric complex of A. DLS of Design C results in a determined molecular weight of 580 ± 407 kDa, suggesting a significantly larger complex than designed; this is consistent with the earlier SEC and gel shift assay results for this complex. Errors in DLS measurements are based on five consecutive measurements of the same sample and reflect the precision of the instrument and not the distribution of the species present.

DISCUSSION

In this work, we set out to develop methods to conjugate short ssDNA strands to proteins so that we could induce selective complex formation between the proteins in a thermally controllable manner. Three designs were pursued: A and B which rely on additional complementary ssDNA strand to link the two separate ssDNA–protein conjugates to one another and C which uses complementary ssDNA strands on each target protein.

In Design A, an omega architecture complex, the titration, DLS, SEC, and gel-shift assay data support the conclusion that a complex is being formed between the two proteins and the ssDNA linker. Despite this evidence for the formation of the desired Design A complex, no FRET is observed between the two fluorescent proteins. The Förster radius for the ECFP/EYFP FRET pairs (50% transfer efficiency) is 4.9 nm.[22] When a practical FRET detection limit of 5% is assumed, the maximum distance between the FRET pair ECFP-EYFP that can be detected is 8 nm.[23] Thus, in Design A, FRET would be expected to be weakly observable, as the EYFP and ECFP are within the 6.8 nm afforded by the DNA linker. We thus speculate that the absence of heteroFRET between EYFP and ECFP in this complex results from the orientational dependence of FRET. This is consistent with the findings of Iqbal et al., who reported a strong dependence on the efficiency of FRET between Cy3 and Cy5 terminally attached to double-stranded nucleic acids arising from the periodicity and length of the DNA strand due to the dependence on the orientation factor (κ) of FRET.[24] This poses a number of issues, however, for the use of Design A for thermal control of complex formation. First, the orientation of the two proteins with respect to one another can be controlled by either increasing or decreasing the length of the DNA strands. Increasing the length of the DNA would increase the melting temperature of the dsDNA complex (negating one of the key design aims of this work), while shortening the strands may in principal work, but as we have seen with our work on design C, shortening the strands weakens the complex and in turn reduces the complex T_m toward room temperature (for a 7bp DNA). This is likely to be unsuitable for many applications. Design A may therefore be considered for applications where the orientation of the two proteins is unimportant.

In the omega architecture Design B where the fluorophores are designed to be held significantly closer, DLS of the mixture reveals an increase in the size of the species present but not to the same extent as observed for Designs A and C; FRET is not observed and native PAGE reveals a greater electrophoresis mobility of the species present compared to the control. We interpret these results as indicating that in Design B the DNA–protein conjugates can hybridize individually to the DNA linker generating an intermediate monohybridized complex of increased molecular weight and net negative charge. Once this monohybridized complex has formed, however, the partner DNA–protein conjugate is unable to bind, perhaps as a result of steric clashes between the proteins. Such steric clashes between the proteins in this arrangement might be relieved by increasing the spacer distance between the two proteins (currently 2 bp, 18 Å space between the ssDNA fragments) at the cost of increased flexibility of the complex.

Our final strategy, the end-of-helix design C, was developed to try to overcome these limitations which relied upon both proteins being conjugated to the opposite termini of complementary ssDNA and thus the proteins at the same end of the dsDNA. Although a much simpler design, this method was successful in bringing the proteins together and enabling FRET. Tests of the lengths of DNA linker used were undertaken which suggests that lengths of 10 bp (24 H-bonds) are necessary for conjugation at room temperature. Shorter GC-only oligonucleotides are likely to permit shorter lengths to be used if linker length is of concern.

Unlike Design A, however, the SEC, DLS, and gel shift assays are consistent with the formation of not only the desired heterodimer, but also a complex of larger size (or more likely a mixture of complexes). The exact nature of this larger oligomer is, however, ambiguous. The complex forms only when the ssDNA strands are complementary to one another. An early supposition of ours was that if the proteins were diconjugated with ssDNA rather than monoconjugated, then a larger oligomeric complex would form. MALDI mass spectrometry of the ssDNA–protein conjugates, however, shows only the desired monoconjugated proteins. The oligomerization of the GFP family of proteins is well-known and has led to the wide adoption of the A206 K mutation, originally reported by Zacharias et al.[16] within applications of these proteins. In this work Zacharias demonstrated that although the mutant has limited affinity for itself compared with wild-type GFP and is thus effectively monomeric in solution, bringing the proteins together in the plasma membrane (by acylation) caused the "monomeric" mutant GFPs to cluster together. These clusters could not be reversed upon disruption of the plasma membrane. Suzuki et al. have demonstrated that the "monomerizing" A206 K mutant EYFP is still capable of generating higher-order oligomers when targeted to the endoplasmic reticulum during expression.[25] Although the complexes observed by Suzuki et al. rely upon disulfide bond formation to hold them together, the oligomerization was found to be due to an inherent oligomerization tendency of the GFP family of proteins. It should be noted that the oligomers observed by Suzuki et al. are not fluorescent, while the complex(es) we observe are. Covalent association of the proteins (for instance, through disulfide bond formation) can be ruled out in this work, as the sole surface-accessible cysteine is the site of DNA hybridization. Importantly, the formation of this complex is reversible, with FRET being eliminated along with protein separation upon melting of the short-length hybridized DNA. It is possible that dimerization forms a new interaction interface which can interact with further proteins, which is the likely source of the higher-order species observed for wild-type GFP.

It is notable that the melting temperature for the hybridized complex was greater than that predicted for the DNA strands on their own—suggesting that the proteins may stabilize the complex in addition to the DNA. We speculate that this arises from nonspecific interactions between the proteins that, although insufficient to hold the complex together on their

DOI: 10.1021/bc500473s
Bioconjugate Chem. 2015, 26, 427–434

own at room temperature, contribute favorably to the attraction of the complex. Controls with noncomplementary DNA linked proteins do not show FRET on their own. We therefore conclude that the higher-order complex observed with Design C is due to the choice of two proteins with some degree of intrinsic aggregation ability, and, although mitigated by the A206 K dimer breaking mutation on both proteins, complex formation (via DNA hybridization) exacerbates the formation of the higher-order species. Such behavior has been suggested previously by Landgraf et al., who noted the formation of fluorescent homo-oligomers in cellular imaging applications. The formation of these oligomers was suggested to result from the fused fluorescent proteins acting as scaffolds preventing individual components from diffusing apart and driving the tagged proteins to coalesce.[26]

We find no evidence for higher-order complexes arising in Design A despite the formation of the desired heterodimeric complex. It is our opinion that in Design A the proteins are sufficiently far apart that they do not physically interact in the same manner as in Design C. Given the inherent oligomerization of EYFP and ECFP, further biophysical characterization of Design C is clearly warranted with other partner proteins.

CONCLUSIONS

In summary, we have demonstrated the reversible assembly of DNA−protein conjugates based on short length of oligonucleotides. Two designs were found to yield complexes (Designs A and C) herein: of these, Design A appears to form a monodisperse and stable complex but in an orientation where FRET cannot occur. Design C also forms the desired complex, however, the inherent tendency of the model proteins EYFP and ECFP to oligomerize results in a previously reported scaffolding effect that drives the association of the heterodimeric complex into a higher-order species.

As an alternative to thermally controlled duplex formation, Yuo et al. have used a light-responsive azobenzene-integrated DNA duplex to control a glucose oxidase (GOx)/horseradish peroxidase (HRP) protein enzyme cascade.[27] Furthermore, Dohno and co-workers have demonstrated the use of a photoswitchable ligand to control the hybridization of ssDNA strands that contain mismatches.[28,29] Such DNA complexes may also find use in applications such as those presented herein and may allow the construction of switchable DNA-based nanoarchitectures.

Although this methodology has been demonstrated for a two-protein system, the two remaining underivatized termini of the ssDNA strands are expected to allow the preparation of more complex assemblies. This, combined with the ability to dynamically control complex formation, holds promise for future applications of very short DNA fragments in biomacromolecular complex formation.

EXPERIMENTAL SECTION

Protein Mutagenesis, Expression, and Purification. Mutations were introduced into both EYFP and ECFP sequentially using the QuikChange method using pET28-based plasmids of ECFP and EYFP as templates. Mutagenic primers were designed following the recommendations according to length and GC content of the QuikChange mutagenesis strategy from Stratagene for site-directed mutagenesis. The presence of the desired mutations was confirmed by DNA sequencing.

The above mutant proteins were expressed in *E. coli* strain Bl21(DE3) using IPTG induction as standard for pET based plasmids. The soluble EYFP and ECFP were purified from cell lysate using an affinity nickel resin column, Ni-NTA Superflow as standard. A second polishing purification step by size exclusion chromatography (on a Superdex 200 column) was used to remove any remaining contaminant proteins present after the affinity purification step. Protein purity was confirmed by SDS-PAGE.

Preparation of DNA Protein Conjugates. Throughout this work ssDNA concentration was calculated by UV spectroscopy using extinction coefficients calculated using Biopolymercalc2.[30] The NHS bearing cross-linker BMPS was used to generate maleimide-ssDNA used for protein labeling.

Modification of Amino ssDNA with NHS-Maleimide Cross-Linker. Amino ssDNA (final concentration 200 μM) was mixed with a 50-fold molar excess of *N*-β-Maleimido propyl-oxysuccinimide ester (BMPS, length 5.9 A, Pierce, 10 mM) in freshly prepared sodium carbonate buffer (200 mM, pH 8.7). This buffer is non-nucleophilic and the pH is very important both to ensure the selectivity of the coupling reaction and to prevent hydrolysis of the NHS group. The reaction was incubated for 1 h at 4 °C and the DNA was purified from the excess cross-linker by using Glen Gel-Pak Desalting Column (Glen Research Corporation) equilibrated in water. The final sample volume was reduced on a Speed-Vac at 50 °C. Final purified yield of the reaction varied between 50% and 70%.

Conjugation of the Maleimide-ssDNA with the Fluorescent Protein. Protein concentrations were established by UV spectrometry (extinction coefficients listed in Supporting Information Table S3). Fluorescent protein (ECFP or EYFP, 50 μM) was mixed with a 4-fold molar excess of maleimide-ssDNA (200 μM) in PBS buffer (pH 7.4) for 5 h at 4 °C. The reaction mixture was then purified by gel filtration chromatography on a Superdex 200 10/300 column equilibrated in PBS buffer. Product containing fractions were concentrated using a spin concentrator. The purified yield of the reaction varied between 20% and 40% calculated with respect to the amount of nanomoles of protein used in the conjugation reaction. The efficiency of the reaction was judged from the chromatogram and the proportions of the absorbance value specific for the DNA (254 nm) and protein (280 and 430/510 nm) (Supporting Information Table S3) and confirmed by SDS-PAGE and mass spectrometry analysis (Supporting Information Figures S1 and S2).

Native PAGE. Proteins were separated on a NuSep precast gradient gel (4−20% acrylamide) using a Tris/Glycine buffer system. Protein bands were visualized by staining with Coomassie blue.

DLS Measurements. DLS was performed at 20 °C on a Malvern Zetasizer on 10 μM protein solutions in PBS buffer pH 7.4. Prior to DLS measurements, protein solutions were centrifuged to remove any dust. The default settings for protein analysis were used throughout calculated as protein volume fraction.

Size Exclusion Chromatography. SEC was performed at 6 °C on a Superdex 200 (10/300) column and eluted with PBS buffer pH 7.4 (0.5 mL/min). Chromatograms were recorded at 260 nm.

FRET Measurements. Förster resonance energy transfer measurements were made using a Horiba FluoroMax4 and Horiba Fluorolog temperature controllable fluorimeters. The ECFP donor fluorophore was excited at 400 nm and emission

DOI: 10.1021/bc500473s
Bioconjugate Chem. 2015, 26, 427−434

arising through emission of EYFP by FRET was monitored between 450 and 600 nm. FRET measurements were performed in PBS buffer pH 7.4.

■ ASSOCIATED CONTENT

Supporting Information

Details on ssDNA sequences used including extinction coefficients and melting temperature. Additional fluorescent spectra, representative mass spectrometry, DLS traces, fluorescence titration and chromatographic data.This material is available free of charge via the Internet at http://pubs.acs.org.

■ AUTHOR INFORMATION

Corresponding Authors

*E-mail: eliza.ploskon@bristol.ac.uk.
*E-mail: paula.booth@kcl.ac.uk.

Notes

The authors declare no competing financial interest.

■ ACKNOWLEDGMENTS

We thank the EPSRC (EP/H019146/1) for funding as part of the New Directions in Synthetic Biology Sandpit.

■ ABBREVIATIONS

FRET, Förster resonance energy transfer; EYFP, enhanced yellow fluorescent protein; ECFP, enhanced cyan fluorescent protein; ssDNA, single stranded DNA; dsDNA, double stranded DNA; SEC, size exclusion chromatography; DLS, dynamic light scattering

■ REFERENCES

(1) Langer, R., and Tirrell, D. A. (2004) Designing materials for biology and medicine. *Nature 428*, 487−492.
(2) Agapakis, C. M., Boyle, P. M., and Silver, P. A. (2012) Natural strategies for the spatial optimization of metabolism in synthetic biology. *Nat. Chem. Biol. 8*, 527−535.
(3) Hirakawa, H., Haga, T., and Nagamune, T. (2012) Artificial protein complexes for biocatalysis. *Top. Catal. 55*, 1124−1137.
(4) Niemeyer, C. M. (2010) Semisynthetic DNA−protein conjugates for biosensing and nanofabrication. *Angew. Chem., Int. Ed. 49*, 1200−1216.
(5) Axup, J. Y., Bajjuri, K. M., Ritland, M., Hutchins, B. M., Kim, C. H., Kazane, S. A., Halder, R., Forsyth, J. S., Santidrian, A. F., Stafin, K., Lu, Y., Tran, H., Seller, A. J., Biroc, S. L., Szydlik, A., Pinkstaff, J. K., Tian, F., Sinha, S. C., Felding-Habermann, B., Smider, V. V., and Schultz, P. G. (2012) Synthesis of site-specific antibody-drug conjugates using unnatural amino acids. *Proc. Natl. Acad. Sci. U. S. A. 109*, 16101−16106.
(6) Piperberg, G., Wilner, O. I., Yehezkeli, O., Tel-Vered, R., and Willner, I. (2009) Control of bioelectrocatalytic transformations on DNA scaffolds. *J. Am. Chem. Soc. 131*, 8724−8725.
(7) Erkelenz, M., Kuo, C. H., and Niemeyer, C. M. (2011) DNA-mediated assembly of cytochrome P450 BM3 subdomains. *J. Am. Chem. Soc. 133*, 16111−16118.
(8) Wilner, O. I., Weizmann, Y., Gill, R., Lioubashevski, O., Freeman, R., and Willner, I. (2009) Enzyme cascades activated on topologically programmed DNA scaffolds. *Nat. Nanotechnol. 4*, 249−254.
(9) Gholami, Z., Brunsveld, L., and Hanley, Q. (2013) PNA-induced assembly of fluorescent proteins using DNA as a framework. *Bioconjugate Chem. 24*, 1378−1386.
(10) Gartner, Z. J., and Liu, D. R. (2001) The generality of DNA-templated synthesis as a basis for evolving non-natural small molecules. *J. Am. Chem. Soc. 123*, 6961−6963.
(11) McKee, M. L., Evans, A. C., Gerrard, S. R., O'Reilly, R. K., Turberfield, A. J., and Stulz, E. (2011) Peptidomimetic bond formation by DNA-templated acyl transfer. *Org. Biomol. Chem. 9*, 1661−1666.
(12) McKee, M. L., Milnes, P. J., Bath, J., Stulz, E., Turberfield, A. J., and O'Reilly, R. K. (2010) Multistep DNA-templated reactions for the synthesis of functional sequence controlled oligomers. *Angew. Chem., Int. Ed. 49*, 7948−7951.
(13) Gartner, Z. J., Grubina, R., Calderone, C. T., and Liu, D. R. (2003) Two enabling architectures for DNA-templated organic synthesis. *Angew. Chem., Int. Ed. 42*, 1370−1375.
(14) Gholami, Z., and Hanley, Q. (2014) Controlled assembly of SNAP-PNA-fluorophore systems on DNA templates to produce fluorescence resonance energy transfer. *Bioconjugate Chem. 25*, 1820−1828.
(15) Yang, F., Moss, L. G., and Phillips, G. N. (1996) The molecular structure of green fluorescent protein. *Nat. Biotechnol. 14*, 1246−1251.
(16) Zacharias, D. A., Violin, J. D., Newton, A. C., and Tsien, R. Y. (2002) Partitioning of lipid-modified monomeric GFPs into membrane microdomains of live cells. *Science 296*, 913−916.
(17) Kukolka, F., and Niemeyer, C. M. (2004) Synthesis of fluorescent oligonucleotide–EYFP conjugate: towards supramolecular construction of semisynthetic biomolecular antennae. *Org. Biomol Chem. 2*, 2203−2206.
(18) Inouye, S., and Tsuji, F. I. (1994) Evidence for redox forms of the Aequorea green fluorescent protein. *FEBS Lett. 351*, 211−214.
(19) Goodman, J. L., Fried, D. B., and Schepartz, A. (2009) Bipartite tetracysteine display requires site flexibility for ReAsH coordination. *ChemBioChem 10*, 1644−1647.
(20) Shaner, N. C., Steinbach, P. A., and Tsien, R. Y. (2005) A guide to choosing fluorescent proteins. *Nat. Methods 2*, 905−909.
(21) Kibbe, W. A. (2007) OligoCalc: an online oligonucleotide properties calculator. *Nucleic Acids Res. 35*, W43−46.
(22) Patterson, G. H., Piston, D. W., and Barisas, B. G. (2000) Förster distances between green fluorescent protein pairs. *Anal. Biochem. 284*, 438−440.
(23) Ganesan, S., Ameer-Beg, S. M., Ng, T. T., Vojnovic, B., and Wouters, F. S. (2006) A dark yellow fluorescent protein (YFP)-based Resonance Energy-Accepting Chromoprotein (REACh) for Förster resonance energy transfer with GFP. *Proc. Natl. Acad. Sci. U. S. A. 103*, 4089−4094.
(24) Iqbal, A., Arslan, S., Okumus, B., Wilson, T. J., Giraud, G., Norman, D. G., Ha, T., and Lilley, D. M. (2008) Orientation dependence in fluorescent energy transfer between Cy3 and Cy5 terminally attached to double-stranded nucleic acids. *Proc. Natl. Acad. Sci. U. S. A. 105*, 11176−11181.
(25) Suzuki, T., Arai, S., Takeuchi, M., Sakurai, C., Ebana, H., Higashi, T., Hashimoto, H., Hatsuzawa, K., and Wada, I. (2012) Development of cysteine-free fluorescent proteins for the oxidative environment. *PLoS One 7*, e37551.
(26) Landgraf, D., Okumus, B., Chien, P., Baker, T. A., and Paulsson, J. (2012) Segregation of molecules at cell division reveals native protein localization. *Nat. Methods 9*, 480−482.
(27) You, M., Wang, R. W., Zhang, X., Chen, Y., Wang, K., Peng, L., and Tan, W. (2011) Photon-regulated DNA-enzymatic nanostructures by molecular assembly. *ACS Nano 5*, 10090−10095.
(28) Dohno, C., Uno, S. N., and Nakatani, K. (2007) Photo-switchable molecular glue for DNA. *J. Am. Chem. Soc. 129*, 11898−11899.
(29) Dohno, C., and Nakatani, K. (2011) Control of DNA hybridization by photoswitchable molecular glue. *Chem. Soc. Rev. 40*, 5718−5729.
(30) Williamson, J. R. *Oligo Extinction Coefficient Calculator*.

DOI: 10.1021/bc500473s
Bioconjugate Chem. 2015, 26, 427−434